Supplemental Material: Synthetic Gauge Field for Two-Dimensional Time-Multiplexed Quantum Random Walks

In the first section of this supplemental material, we explain the experimental details. The details of the theoretical analysis are summarized in the subsequent section.

I. EXPERIMENTAL DETAILS:

For the purpose of pulse generation in this quantum walk experiment, we used a laser diode operating at the C-band of the telecom wavelength (1550 nm). By modulation of this laser made by Bookham technology (LC25W5172BA-J34), we generated pulses with a power of $10\,mW$ and a pulse duration of two nanoseconds. These pulses are sent into the setup with a repetition rate of $10\,\mu s$. We used these pulses to initiate the quantum walk in our synthetic two-dimensional space. Moreover, the polarization of the incident pulse is controlled using the polarization beam splitter.

Figure 1b in the manuscript shows the experimental setup used for making the synthetic two-dimensional space. The initial pulse after passing through the first 50/50 beam splitter chooses to continue its path through either the 1 m or 2 m fiber length. This leads to different delays that can be regarded as choosing the left or right direction in the x movement. By reaching the next beam splitter, the pulse chooses either the 130 m or 118 m fiber spool. This determines whether the pulse has gone to the up or down direction in the y movement. In this way, we encode the x and y movement of the pulses based on the delay in reaching the detectors. We used 90/10 beam splitters to out-couple 10% of the light for detection purposes.

In order to compensate for the loss in the experimental setup, we used semiconductor optical amplifiers made by Thorlabs (SOA1117S). These amplifiers, which are turned on for a fraction of a repetition period at each cycle, provide the capability to amplify the pulses without ruining their phase coherence. However, in addition to amplifying the signal they increase the background noise due to spontaneous emission. Such noises should be filtered out using band-pass filters. For this purpose, we used narrow band-pass filters ($< 0.3\,nm$) right after the semiconductor optical amplifiers, as shown in Fig. 1b.

Despite this compensation, the ratio of the optical pulse power at different positions of the synthetic space relative to the noise degrades with increasing time steps due to the diffusion and the added noise. Because of the degradation of the signal-to-noise ratio and the finite ratio of the time delays corresponding to the x and y movements, we limited our measurement of the quantum walk distribution to 10 steps. By measuring the power of the pulses present in each step, we can determine the distribution of the quantum walk at every time step.

In addition, the polarization of the incident pulse varies by passing through the fiber network. To compensate for these polarization changes, we used polarization controllers in our setup.

Furthermore, we used two phase modulators in this setup that apply opposite phases to the left and right moving pulses. These phase modulators (MPZ-LN-10-P-P-FA-FA) made by Cybel company can provide a switching speed of $12\,Gb/s$ and have $3\,dB$ loss.

We note that the error in our measurement of the intensity of the pulses at different time delays (corresponding to

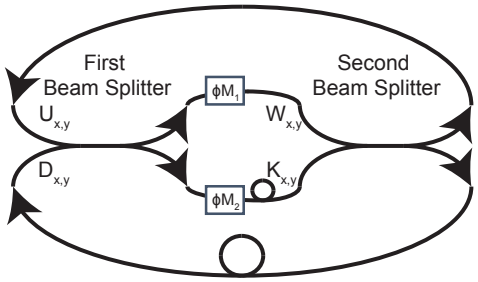

Figure S1. Simplified version of the schematic of the two-dimensional quantum walk setup.

different positions in the synthetic space) is around 3% ($\Delta P_{x,y}/P_{x,y} = 3\%$). This error will propagate to the error in the calculated quadratic means, as explained in the following.

By defining $P_1 = \sum_{x,y} x^2 P_{x,y}$ and $P_2 = \sum_{x,y} P_{x,y}$, in which $P_{x,y}$ is the power detected at coordinates x and y in the synthetic space, the quadratic mean of x is calculated based on:

$$x_{rms} = \sqrt{< x^2 >} = \sqrt{\frac{\sum_{x,y} x^2 P_{x,y}}{\sum_{x,y} P_{x,y}}} = \sqrt{\frac{P_1}{P_2}}$$

By assuming that $\Delta P_{x,y}/P_{x,y} = D = 3\%$, since $x^2 > 0$ and $P_{x,y} > 0$, then:

$$\frac{\Delta P_1}{P_1} = \frac{\sqrt{\sum_{x,y} x^4 \left(\Delta P_{x,y}\right)^2}}{\sum_{x,y} x^2 P_{x,y}} = \frac{D\sqrt{\sum_{x,y} x^4 P_{x,y}^2}}{\sum x^2 P_{x,y}} \leq D$$

$$\frac{\Delta P_2}{P_2} = \frac{\sqrt{\sum_{x,y} \left(\Delta P_{x,y}\right)^2}}{\sum_{x,y} P_{x,y}} = \frac{D\sqrt{\sum_{x,y} P_{x,y}^2}}{\sum_{x,y} P_{x,y}} \leq D$$

Therefore:

$$\frac{\Delta < x^2 >}{< x^2 >} = \sqrt{\left(\frac{\Delta P_1}{P_1}\right)^2 + \left(\frac{\Delta P_2}{P_2}\right)^2} \leq \sqrt{2} D$$

Consequently:

$$\frac{\Delta x_{rms}}{x_{rms}} = \frac{1}{2}\frac{\Delta < x^2 >}{< x^2 >} \leq \frac{1}{\sqrt{2}} D$$

A similar analysis holds for the y direction. Therefore, the error bars in the quadratic means are less than 3% and are smaller than the size of the plotted data points in the manuscript.

II. THEORETICAL ANALYSIS:

In the following, the evolution of pulses (representing the quantum walkers) in the two-dimensional quantum walk is analyzed. For the theoretical analysis of the quantum walk, we can assume that all the losses in the setup, including the losses caused by the 90/10 beam splitters as well as phase modulators, are fully compensated by the amplifiers. Moreover, we can assume that polarization controllers compensate for the polarization changes in the setup. Therefore, we can simplify the schematic for theoretical analysis and consider an ideal setup as shown in Fig. S1.

Two pulses just before the first beam splitter, $\begin{bmatrix} U_{x,y}^{(n)} \\ D_{x,y}^{(n)} \end{bmatrix}$, will produce the output pulses as (movement in the x direction):

$$\begin{bmatrix} W_{x-1,y} \\ K_{x+1,y} \end{bmatrix} = \frac{1}{\sqrt{2}} \begin{bmatrix} e^{i\phi_{n,y}} & 0 \\ 0 & e^{-i\phi_{n,y}} \end{bmatrix} \begin{bmatrix} 1 & -1 \\ 1 & 1 \end{bmatrix} \begin{bmatrix} U_{x,y}^{(n)} \\ D_{x,y}^{(n)} \end{bmatrix}.$$

Note that the applied phases are assumed to be explicit functions of the time step (n) as well as y coordinate but not x coordinate due to experimental limitations.

Pulses which are input to the second beam splitter, $\begin{bmatrix} W_{x,y} \\ K_{x,y} \end{bmatrix}$, will produce the outputs as (movement in the y direction):

$$\begin{bmatrix} U_{x,y+1}^{(n+1)} \\ D_{x,y-1}^{(n+1)} \end{bmatrix} = \frac{1}{\sqrt{2}} \begin{bmatrix} 1 & -1 \\ 1 & 1 \end{bmatrix} \begin{bmatrix} W_{x,y} \\ K_{x,y} \end{bmatrix}$$

By considering the pulse of $\begin{bmatrix} W_{x-1,y} \\ 0 \end{bmatrix}$ caused by $\begin{bmatrix} U_{x,y}^{(n)} \\ D_{x,y}^{(n)} \end{bmatrix}$, we have:

$$\begin{aligned} \begin{bmatrix} U_{x-1,y+1}^{(n+1)} \\ D_{x-1,y-1}^{(n+1)} \end{bmatrix} &= \frac{1}{\sqrt{2}} \begin{bmatrix} 1 & -1 \\ 1 & 1 \end{bmatrix} \begin{bmatrix} W_{x-1,y} \\ 0 \end{bmatrix} \\ &= \frac{1}{2} \begin{bmatrix} 1 & -1 \\ 1 & 1 \end{bmatrix} \begin{bmatrix} 1 & 0 \\ 0 & 0 \end{bmatrix} \begin{bmatrix} e^{i\phi_{n,y}} & 0 \\ 0 & e^{-i\phi_{n,y}} \end{bmatrix} \begin{bmatrix} 1 & -1 \\ 1 & 1 \end{bmatrix} \begin{bmatrix} U_{x,y}^{(n)} \\ D_{x,y}^{(n)} \end{bmatrix} \\ &= \frac{1}{2} \begin{bmatrix} e^{i\phi_{n,y}} & -e^{i\phi_{n,y}} \\ e^{i\phi_{n,y}} & -e^{i\phi_{n,y}} \end{bmatrix} \begin{bmatrix} U_{x,y}^{(n)} \\ D_{x,y}^{(n)} \end{bmatrix} \end{aligned}$$

Furthermore, by considering the pulse of $\begin{bmatrix} 0 \\ K_{x+1,y} \end{bmatrix}$ caused by $\begin{bmatrix} U_{x,y}^{(n)} \\ D_{x,y}^{(n)} \end{bmatrix}$, we have:

$$\begin{aligned} \begin{bmatrix} U_{x+1,y+1}^{(n+1)} \\ D_{x+1,y-1}^{(n+1)} \end{bmatrix} &= \frac{1}{\sqrt{2}} \begin{bmatrix} 1 & -1 \\ 1 & 1 \end{bmatrix} \begin{bmatrix} 0 \\ K_{x+1,y} \end{bmatrix} \\ &= \frac{1}{2} \begin{bmatrix} 1 & -1 \\ 1 & 1 \end{bmatrix} \begin{bmatrix} 0 & 0 \\ 0 & 1 \end{bmatrix} \begin{bmatrix} e^{i\phi_{n,y}} & 0 \\ 0 & e^{-i\phi_{n,y}} \end{bmatrix} \begin{bmatrix} 1 & -1 \\ 1 & 1 \end{bmatrix} \begin{bmatrix} U_{x,y}^{(n)} \\ D_{x,y}^{(n)} \end{bmatrix} \\ &= \frac{1}{2} \begin{bmatrix} -e^{-i\phi_{n,y}} & -e^{-i\phi_{n,y}} \\ e^{-i\phi_{n,y}} & e^{-i\phi_{n,y}} \end{bmatrix} \begin{bmatrix} U_{x,y}^{(n)} \\ D_{x,y}^{(n)} \end{bmatrix} \end{aligned}$$

Therefore, $\begin{bmatrix} U_{x,y}^{(n)} \\ D_{x,y}^{(n)} \end{bmatrix}$ will produce the following pulses after traversing both of the beam splitters:

$$U_{x-1,y+1}^{(n+1)} = \frac{1}{2} \left(e^{i\phi_{n,y}} U_{x,y}^{(n)} - e^{i\phi_{n,y}} D_{x,y}^{(n)} \right)$$

$$U_{x+1,y+1}^{(n+1)} = \frac{1}{2}\left(-e^{-i\phi_{n,y}}U_{x,y}^{(n)} - e^{-i\phi_{n,y}}D_{x,y}^{(n)}\right)$$

$$D_{x-1,y-1}^{(n+1)} = \frac{1}{2}\left(e^{i\phi_{n,y}}U_{x,y}^{(n)} - e^{i\phi_{n,y}}D_{x,y}^{(n)}\right)$$

$$D_{x+1,y-1}^{(n+1)} = \frac{1}{2}\left(e^{-i\phi_{n,y}}U_{x,y}^{(n)} + e^{-i\phi_{n,y}}D_{x,y}^{(n)}\right)$$

Alternatively, based on the above results $\begin{bmatrix} U_{x,y}^{(n+1)} \\ D_{x,y}^{(n+1)} \end{bmatrix}$ can be produced from other pulses as:

$$U_{x,y}^{(n+1)} = \frac{e^{i\phi_{n,y-1}}}{2}\left(U_{x+1,y-1}^{(n)} - D_{x+1,y-1}^{(n)}\right) - \frac{e^{-i\phi_{n,y-1}}}{2}\left(U_{x-1,y-1}^{(n)} + D_{x-1,y-1}^{(n)}\right)$$

$$D_{x,y}^{(n+1)} = \frac{e^{i\phi_{n,y+1}}}{2}\left(U_{x+1,y+1}^{(n)} - D_{x+1,y+1}^{(n)}\right) + \frac{e^{-i\phi_{n,y+1}}}{2}\left(U_{x-1,y+1}^{(n)} + D_{x-1,y+1}^{(n)}\right)$$

The above two equations fully describe the evolution of the pulses. We can prove that any constant phase independent of the time step and coordinate will not change the dynamics the of evolution. For this purpose, we separate out any such constant phase from $\phi_{n,y}$ and we assume that $\phi_{n,y}$ can be written as:

$$\phi_{n,y} = \Phi + \phi'_{n,y}$$

Therefore:

$$U_{x,y}^{(n+1)} = \frac{e^{i\Phi+i\phi'_{n,y-1}}}{2}\left(U_{x+1,y-1}^{(n)} - D_{x+1,y-1}^{(n)}\right) - \frac{e^{-i\Phi-i\phi'_{n,y-1}}}{2}\left(U_{x-1,y-1}^{(n)} + D_{x-1,y-1}^{(n)}\right)$$

$$D_{x,y}^{(n+1)} = \frac{e^{i\Phi+i\phi'_{n,y+1}}}{2}\left(U_{x+1,y+1}^{(n)} - D_{x+1,y+1}^{(n)}\right) + \frac{e^{-i\Phi-i\phi'_{n,y+1}}}{2}\left(U_{x-1,y+1}^{(n)} + D_{x-1,y+1}^{(n)}\right)$$

By defining U' and D' from U and D as:

$$U'^{(n)}_{x,y} = e^{ix\Phi}U_{x,y}^{(n)}$$

$$D'^{(n)}_{x,y} = e^{ix\Phi}D_{x,y}^{(n)}$$

We have:

$$U'^{(n+1)}_{x,y} = \frac{e^{i\phi'_{n,y-1}}}{2}\left(U'^{(n)}_{x+1,y-1} - D'^{(n)}_{x+1,y-1}\right) - \frac{e^{-i\phi'_{n,y-1}}}{2}\left(U'^{(n)}_{x-1,y-1} + D'^{(n)}_{x-1,y-1}\right)$$

$$D'^{(n+1)}_{x,y} = \frac{e^{i\phi'_{n,y+1}}}{2}\left(U'^{(n)}_{x+1,y+1} - D'^{(n)}_{x+1,y+1}\right) + \frac{e^{-i\phi'_{n,y+1}}}{2}\left(U'^{(n)}_{x-1,y+1} + D'^{(n)}_{x-1,y+1}\right)$$

This shows that the evolution is invariant under such a constant phase application.
By defining $S_{x,y}^{(n)} = U_{x,y}^{(n)} + D_{x,y}^{(n)}$ and $P_{x,y}^{(n)} = U_{x,y}^{(n)} - D_{x,y}^{(n)}$, the obtained equations can be written as:

$$\begin{bmatrix} S_{x,y}^{(n+1)} \\ P_{x,y}^{(n+1)} \end{bmatrix} = \frac{1}{2} \begin{bmatrix} e^{-i\phi_{n,y+1}} & e^{i\phi_{n,y+1}} & -e^{-i\phi_{n,y-1}} & e^{i\phi_{n,y-1}} \\ -e^{-i\phi_{n,y+1}} & -e^{i\phi_{n,y+1}} & -e^{-i\phi_{n,y-1}} & e^{i\phi_{n,y-1}} \end{bmatrix} \begin{bmatrix} S_{x-1,y+1}^{(n)} \\ P_{x+1,y+1}^{(n)} \\ S_{x-1,y-1}^{(n)} \\ P_{x+1,y-1}^{(n)} \end{bmatrix}$$

Now that we have the governing equation in the real space, we can think about its solution in the Fourier space. By defining $s_{k_x,k_y}^{(n)}$ and $p_{k_x,k_y}^{(n)}$ as Fourier transforms of $S_{x,y}^{(n)}$ and $P_{x,y}^{(n)}$, we have:

$$\begin{bmatrix} S_{x,y}^{(n)} \\ P_{x,y}^{(n)} \end{bmatrix} = \frac{1}{4\pi^2} \begin{bmatrix} \int\int_{k_x,k_y} s_{k_x,k_y}^{(n)} e^{ik_x x + ik_y y} dk_x dk_y \\ \int\int_{k_x,k_y} p_{k_x,k_y}^{(n)} e^{ik_x x + ik_y y} dk_x dk_y \end{bmatrix}$$

Therefore:

$$\begin{bmatrix} \int\int_{k_x,k_y} s_{k_x,k_y}^{(n+1)} e^{ik_x x + ik_y y} dk_x dk_y \\ \int\int_{k_x,k_y} p_{k_x,k_y}^{(n+1)} e^{ik_x x + ik_y y} dk_x dk_y \end{bmatrix} = \frac{1}{2} \begin{bmatrix} e^{-i\phi_{n,y+1}} & e^{i\phi_{n,y+1}} & -e^{-i\phi_{n,y-1}} & e^{i\phi_{n,y-1}} \\ -e^{-i\phi_{n,y+1}} & -e^{i\phi_{n,y+1}} & -e^{-i\phi_{n,y-1}} & e^{i\phi_{n,y-1}} \end{bmatrix}$$
$$\times \begin{bmatrix} \int\int_{k_x,k_y} e^{ik_y - ik_x} s_{k_x,k_y}^{(n)} e^{ik_x x + ik_y y} dk_x dk_y \\ \int\int_{k_x,k_y} e^{ik_x + ik_y} p_{k_x,k_y}^{(n)} e^{ik_x x + ik_y y} dk_x dk_y \\ \int\int_{k_x,k_y} e^{-ik_x - ik_y} s_{k_x,k_y}^{(n)} e^{ik_x x + ik_y y} dk_x dk_y \\ \int\int_{k_x,k_y} e^{ik_x - ik_y} p_{k_x,k_y}^{(n)} e^{ik_x x + ik_y y} dk_x dk_y \end{bmatrix}$$

This equation can be used to solve the Fourier transforms as functions of the time step. In the following subsections, we solve this equation for two cases of no phase modulation as well as time-independent linear phase modulation.

A. Zero phase modulation:

For the case of no applied phase modulation, we have:

$$\begin{bmatrix} s^{(n+1)}_{k_x,k_y} \\ p^{(n+1)}_{k_x,k_y} \end{bmatrix} = \begin{bmatrix} ie^{-ik_x}\sin(k_y) & e^{ik_x}\cos(k_y) \\ -e^{-ik_x}\cos(k_y) & -ie^{ik_x}\sin(k_y) \end{bmatrix} \begin{bmatrix} s^{(n)}_{k_x,k_y} \\ p^{(n)}_{k_x,k_y} \end{bmatrix}$$

Note that the evolution matrix has the determinant of 1. Based on this matrix, the effective Hamiltonian, $H_{eff} = i\log(U)$, is given by:

$$H = \begin{pmatrix} -\cos(k_x)\sin(k_y) & ie^{ik_x}\cos(k_y) \\ -ie^{-ik_x}\cos(k_y) & \cos(k_x)\sin(k_y) \end{pmatrix} \frac{\arccos(\sin(k_x)\sin(k_y))}{\sin(\arccos(\sin(k_x)\sin(k_y)))}$$

The obtained Hamiltonian is obviously Hermitian. The eigenvalues of this Hamiltonian are given by:

$$E_{\pm} = \pm\arccos(\sin(k_x)\sin(k_y))$$

Moreover, the eigenvectors are given by:

$$\begin{pmatrix} \cos(k_x)\sin(k_y) \mp \sqrt{1-\sin^2(k_x)\sin^2(k_y)} \\ ie^{-ik_x}\cos(k_y) \end{pmatrix}$$

Therefore, by defining S as

$$S = \begin{pmatrix} \cos(k_x)\sin(k_y) - \sqrt{1-\sin^2(k_x)\sin^2(k_y)} & \cos(k_x)\sin(k_y) + \sqrt{1-\sin^2(k_x)\sin^2(k_y)} \\ ie^{-ik_x}\cos(k_y) & ie^{-ik_x}\cos(k_y) \end{pmatrix},$$

we can write the Hamiltonian as:

$$H = S \begin{pmatrix} E_+ & 0 \\ 0 & E_- \end{pmatrix} S^{-1}$$

Based on the obtained eigen-energies, the band diagram for the zero phase modulation has been plotted in Fig. 3c. The evolution after n steps is described by:

$$\begin{aligned} \begin{bmatrix} s^{(n)}_{k_x,k_y} \\ p^{(n)}_{k_x,k_y} \end{bmatrix} &= \begin{bmatrix} ie^{-ik_x}\sin(k_y) & e^{ik_x}\cos(k_y) \\ -e^{-ik_x}\cos(k_y) & -ie^{ik_x}\sin(k_y) \end{bmatrix}^n \begin{bmatrix} s^{(0)}_{k_x,k_y} \\ p^{(0)}_{k_x,k_y} \end{bmatrix} \\ &= U^n \begin{bmatrix} s^{(0)}_{k_x,k_y} \\ p^{(0)}_{k_x,k_y} \end{bmatrix} \end{aligned}$$

The deterministic equation for the evolution matrix, $\lambda^2 - 2\lambda\sin(k_y)\sin(k_x) + 1 = 0$, gives the following eigenvalues:

$$\lambda_{1,2} = \sin(k_y)\sin(k_x) \mp \sqrt{\sin^2(k_y)\sin^2(k_x) - 1}$$

They are equal to $e^{-iE_{\pm}}$ as we expect. We can define the following two orthogonal functions for calculating the matrix power:

$$e^{(n)}_{k_x,k_y}, f^{(n)}_{k_x,k_y} = e^{-ik_x}\cos(k_y)\, s^{(n)}_{k_x,k_y} + \left(i\cos(k_x)\sin(k_y) \pm \sqrt{\sin^2(k_y)\sin^2(k_x) - 1}\right) p^{(n)}_{k_x,k_y}$$

These functions obey the following independent equations:

$$\begin{aligned} e_{k_x,k_y}^{(n+1)} &= \left(\sin\left(k_x\right)\sin\left(k_y\right) - \sqrt{\sin^2\left(k_y\right)\sin^2\left(k_x\right)-1}\right) e_{k_x,k_y}^{(n)} \\ f_{k_x,k_y}^{(n+1)} &= \left(\sin\left(k_x\right)\sin\left(k_y\right) + \sqrt{\sin^2\left(k_y\right)\sin^2\left(k_x\right)-1}\right) f_{k_x,k_y}^{(n)} \end{aligned}$$

Assuming that the whole evolution is caused by a single pulse at the origin ($U_{x,y}^{(0)} = \delta\left(x\right)\delta\left(y\right)$ and $D_{x,y}^{(0)} = 0$, which are equivalent to $S_{x,y}^{(0)} = \delta\left(x\right)\delta\left(y\right)$ and $P_{x,y}^{(0)} = \delta\left(x\right)\delta\left(y\right)$), then we would have:

$$\begin{bmatrix} s_{k_x,k_y}^{(0)} \\ p_{k_x,k_y}^{(0)} \end{bmatrix} = \begin{bmatrix} 1 \\ 1 \end{bmatrix}$$

Therefore, for the down channel pulses, $d_{k_x,k_y}^{(n)} = 0.5\left(s_{k_x,k_y}^{(n)} - p_{k_x,k_y}^{(n)}\right)$, we have:

$$\begin{aligned} d_{k_x,k_y}^{(n)} &= 0.5\left(s_{k_x,k_y}^{(n)} - p_{k_x,k_y}^{(n)}\right) \\ &= e^{ik_y}\cos\left(k_x\right)\frac{\sin\left(n\arccos\left(\sin\left(k_x\right)\sin\left(k_y\right)\right)\right)}{\sin\left(\arccos\left(\sin\left(k_x\right)\sin\left(k_y\right)\right)\right)} \end{aligned}$$

All the moments, such as the distribution variances and averages ($\left\langle x^2\right\rangle_D$, $\left\langle y^2\right\rangle_D$,$\left\langle x\right\rangle_D$ and $\left\langle y\right\rangle_D$) as functions of the time step n, can be obtained from the above expression.

Based on the fact that:

$$d_{k_x,k_y}^{(n)} = \sum_{x,y} D_{x,y}^{(n)} e^{-ik_x x} e^{-ik_y y}$$

Then:

$$d_{l_x,l_y}^{(n)*} d_{k_x,k_y}^{(n)} = \sum_{p,q}\sum_{x,y} e^{-i(k_x x - l_x p)} e^{-i(k_y y - l_y q)} D_{p,q}^{(n)*} D_{x,y}^{(n)}$$

Therefore, the following equations can be obtained, straightforwardly:

$$\begin{aligned} P_D &= \sum_{x,y}\left|D_{x,y}^{(n)}\right|^2 = \frac{1}{4\pi^2}\int_{k_y=0}^{2\pi}\int_{k_x=0}^{2\pi}\left|d_{k_x,k_y}^{(n)}\right|^2 dk_x dk_y \\ &= \frac{1}{4\pi^2}\int_{k_y=0}^{2\pi}\int_{k_x=0}^{2\pi}\cos^2\left(k_x\right)\frac{\sin^2\left(n\arccos\left(\sin\left(k_x\right)\sin\left(k_y\right)\right)\right)}{\sin^2\left(\arccos\left(\sin\left(k_x\right)\sin\left(k_y\right)\right)\right)} dk_x dk_y \end{aligned}$$

$$\left\langle x\right\rangle_D = \sum_{x,y} x\left|D_{x,y}^{(n)}\right|^2 = \frac{1}{4\pi^2}\int_{k_y=0}^{2\pi}\int_{k_x=0}^{2\pi} d_{k_x,k_y}^{(n)*}\left(i\frac{d}{dk_x}\right) d_{k_x,k_y}^{(n)} dk_x dk_y = 0$$

$$\begin{aligned} \left\langle y\right\rangle_D &= \sum_{x,y} y\left|D_{x,y}^{(n)}\right|^2 = \frac{1}{4\pi^2}\int_{k_y=0}^{2\pi}\int_{k_x=0}^{2\pi} d_{k_x,k_y}^{(n)*}\left(i\frac{d}{dk_y}\right) d_{k_x,k_y}^{(n)} dk_x dk_y \\ &= \frac{-1}{4\pi^2}\int_{k_y=0}^{2\pi}\int_{k_x=0}^{2\pi}\cos^2\left(k_x\right)\frac{\sin^2\left(n\arccos\left(\sin\left(k_x\right)\sin\left(k_y\right)\right)\right)}{\sin^2\left(\arccos\left(\sin\left(k_x\right)\sin\left(k_y\right)\right)\right)} dk_x dk_y = -P_D \end{aligned}$$

$$\begin{aligned}
\left\langle x^2\right\rangle_D &= \sum_{x,y} x^2 \left|D^{(n)}_{x,y}\right|^2 = \frac{1}{4\pi^2}\int_{k_y=0}^{2\pi}\int_{k_x=0}^{2\pi} d^{(n)*}_{k_x,k_y}\left(i\frac{d}{dk_x}\right)^2 d^{(n)}_{k_x,k_y}dk_xdk_y \\
&= \frac{n^2}{4\pi^2}\int_{k_y=0}^{2\pi}\int_{k_x=0}^{2\pi}\frac{\cos^4(k_x)\sin^2(k_y)}{\left(1-\sin^2(k_x)\sin^2(k_y)\right)^2}\sin^2\left(n\cos^{-1}\left(\sin(k_x)\sin(k_y)\right)\right)dk_xdk_y \\
&- \frac{3n}{8\pi^2}\int_{k_y=0}^{2\pi}\int_{k_x=0}^{2\pi}\frac{\sin(k_x)\sin(k_y)\cos^2(k_x)\cos^2(k_y)}{\left(1-\sin^2(k_x)\sin^2(k_y)\right)^{5/2}}\sin\left(2n\cos^{-1}\left(\sin(k_x)\sin(k_y)\right)\right)dk_xdk_y \\
&+ \frac{3}{4\pi^2}\int_{k_y=0}^{2\pi}\int_{k_x=0}^{2\pi}\frac{\sin^2(k_x)\sin^2(k_y)\cos^2(k_x)\cos^2(k_y)}{\left(1-\sin^2(k_x)\sin^2(k_y)\right)^3}\sin^2\left(n\cos^{-1}\left(\sin(k_x)\sin(k_y)\right)\right)dk_xdk_y \\
&+ \frac{1}{4\pi^2}\int_{k_y=0}^{2\pi}\int_{k_x=0}^{2\pi}\frac{\cos^2(k_x)\cos^2(k_y)}{\left(1-\sin^2(k_x)\sin^2(k_y)\right)^2}\sin^2\left(n\cos^{-1}\left(\sin(k_x)\sin(k_y)\right)\right)dk_xdk_y
\end{aligned}$$

$$\begin{aligned}
\left\langle y^2\right\rangle_D &= \sum_{x,y} y^2 \left|D^{(n)}_{x,y}\right|^2 = \frac{1}{4\pi^2}\int_{k_y=0}^{2\pi}\int_{k_x=0}^{2\pi} d^{(n)*}_{k_x,k_y}\left(i\frac{d}{dk_y}\right)^2 d^{(n)}_{k_x,k_y}dk_xdk_y \\
&= \frac{n^2}{4\pi^2}\int_{k_y=0}^{2\pi}\int_{k_x=0}^{2\pi}\frac{\sin^2(k_x)\cos^2(k_x)\cos^2(k_y)}{\left(1-\sin^2(k_x)\sin^2(k_y)\right)^2}\sin^2\left(n\cos^{-1}\left(\sin(k_x)\sin(k_y)\right)\right)dk_xdk_y \\
&+ \frac{n}{4\pi^2}\int_{k_y=0}^{2\pi}\int_{k_x=0}^{2\pi}\frac{\cos^2(k_x)\sin(k_x)\sin(k_y)}{\left(1-\sin^2(k_x)\sin^2(k_y)\right)^{3/2}}\sin\left(2n\cos^{-1}\left(\sin(k_x)\sin(k_y)\right)\right)dk_xdk_y \\
&- \frac{3n}{8\pi^2}\int_{k_y=0}^{2\pi}\int_{k_x=0}^{2\pi}\frac{\cos^4(k_x)\sin(k_x)\sin(k_y)}{\left(1-\sin^2(k_x)\sin^2(k_y)\right)^{5/2}}\sin\left(2n\cos^{-1}\left(\sin(k_x)\sin(k_y)\right)\right)dk_xdk_y \\
&+ \frac{1}{2\pi^2}\int_{k_y=0}^{2\pi}\int_{k_x=0}^{2\pi}\frac{\cos^2(k_x)\left(\sin^2(k_x)\cos^2(k_y)-1\right)}{\left(1-\sin^2(k_x)\sin^2(k_y)\right)^2}\sin^2\left(n\cos^{-1}\left(\sin(k_x)\sin(k_y)\right)\right)dk_xdk_y \\
&+ \frac{3}{4\pi^2}\int_{k_y=0}^{2\pi}\int_{k_x=0}^{2\pi}\frac{\cos^4(k_x)}{\left(1-\sin^2(k_x)\sin^2(k_y)\right)^3}\sin^2\left(n\cos^{-1}\left(\sin(k_x)\sin(k_y)\right)\right)dk_xdk_y
\end{aligned}$$

In the limit of large n, we have:

$$P_D \to \frac{1}{8\pi^2}\int_{k_y=0}^{2\pi}\int_{k_x=0}^{2\pi}\frac{\cos^2(k_x)}{\sin^2\left(\arccos\left(\sin(k_x)\sin(k_y)\right)\right)}dk_xdk_y = \frac{1}{\pi}$$

$$\left\langle x\right\rangle_D \to 0$$

$$\left\langle y\right\rangle_D \to -\frac{1}{\pi}$$

$$\left\langle x^2\right\rangle_D \to \frac{n^2}{8\pi^2}\int_{k_y=0}^{2\pi}\int_{k_x=0}^{2\pi}\frac{\cos^4(k_x)\sin^2(k_y)}{\left(1-\sin^2(k_x)\sin^2(k_y)\right)^2}dk_xdk_y = \frac{n^2}{2\pi}$$

$$\left\langle y^2\right\rangle_D \to \frac{n^2}{8\pi^2}\int_{k_y=0}^{2\pi}\int_{k_x=0}^{2\pi}\frac{\sin^2(k_x)\cos^2(k_x)\cos^2(k_y)}{\left(1-\sin^2(k_x)\sin^2(k_y)\right)^2}dk_xdk_y = \frac{n^2}{6\pi}$$

which shows that $\left\langle y^2\right\rangle_D$ is three times less than $\left\langle x^2\right\rangle_D$. These results prove that the spatial quadratic means of the quantum walk distribution linearly vary with the time step. Note that these average values are normalized relative to

the total power in the up and down channels. However, they can also be normalized relative to the total power present in the corresponding channel. Such a normalization has been used in the manuscript to calculate the experimental and theoretical quadratic means. Since the probabilities of P_D and P_U tend toward constant values, by the latter normalization the asymptotic behavior of the quadratic means remains linear relative to the time step.

It is interesting to test some first steps:

$$d^{(0)}_{k_x,k_y} = 0 \rightarrow D^{(0)}_{x,y} = 0$$

$$d^{(1)}_{k_x,k_y} = e^{ik_y}\cos\left(k_x\right) \rightarrow D^{(1)}_{x,y} = \begin{cases} 0.5\,(x=-1,y=-1) \\ 0.5\,(x=1,y=-1) \\ 0\,(Otherwise) \end{cases}$$

$$d^{(2)}_{k_x,k_y} = e^{ik_y}\sin\left(2k_x\right)\sin\left(k_y\right) \rightarrow D^{(2)}_{x,y} = \begin{cases} -0.25\,(x=-2,y=-2) \\ 0\,(x=0,y=-2) \\ 0.25\,(x=2,y=-2) \\ 0.25\,(x=-2,y=0) \\ 0\,(x=0,y=0) \\ -0.25\,(x=2,y=0) \\ 0\,(Otherwise) \end{cases}$$

$$d^{(3)}_{k_x,k_y} = e^{ik_y}\cos\left(k_x\right)\left(\cos\left(2k_x\right)\cos\left(2k_y\right) - \cos\left(2k_x\right) - \cos\left(2k_y\right)\right) \rightarrow D^{(3)}_{x,y} = \begin{cases} 0.125\,(x=-3,y=-3) \\ -0.125\,(x=-1,y=-3) \\ -0.125\,(x=1,y=-3) \\ 0.125\,(x=3,y=-3) \\ -0.25\,(x=-3,y=-1) \\ -0.25\,(x=-1,y=-1) \\ -0.25\,(x=1,y=-1) \\ -0.25\,(x=3,y=-1) \\ 0.125\,(x=-3,y=1) \\ -0.125\,(x=-1,y=1) \\ -0.125\,(x=1,y=1) \\ 0.125\,(x=3,y=1) \\ 0\,(Otherwise) \end{cases}$$

Similarly, we can investigate the up channel:

$$\begin{aligned} u^{(n)}_{k_x,k_y} &= 0.5\left(s^{(n)}_{k_x,k_y} + p^{(n)}_{k_x,k_y}\right) \\ &= \cos\left(n\arccos\left(\sin\left(k_x\right)\sin\left(k_y\right)\right)\right) + i\cos\left(k_y\right)\sin\left(k_x\right)\frac{\sin\left(n\arccos\left(\sin\left(k_x\right)\sin\left(k_y\right)\right)\right)}{\sin\left(\arccos\left(\sin\left(k_x\right)\sin\left(k_y\right)\right)\right)} \end{aligned}$$

$$\begin{aligned} P_U &= \sum_{x,y}\left|U^{(n)}_{x,y}\right|^2 = \frac{1}{4\pi^2}\int_{k_y=0}^{2\pi}\int_{k_x=0}^{2\pi}\left|u^{(n)}_{k_x,k_y}\right|^2 dk_x dk_y \\ &= \frac{1}{4\pi^2}\int_{k_y=0}^{2\pi}\int_{k_x=0}^{2\pi}\cos^2\left(n\arccos\left(\sin\left(k_x\right)\sin\left(k_y\right)\right)\right)dk_x dk_y \\ &+ \frac{1}{4\pi^2}\int_{k_y=0}^{2\pi}\int_{k_x=0}^{2\pi}\cos^2\left(k_y\right)\sin^2\left(k_x\right)\frac{\sin^2\left(n\arccos\left(\sin\left(k_x\right)\sin\left(k_y\right)\right)\right)}{\sin^2\left(\arccos\left(\sin\left(k_x\right)\sin\left(k_y\right)\right)\right)}dk_x dk_y \end{aligned}$$

$$\left\langle x\right\rangle_U = \sum_{x,y} x\left|U^{(n)}_{x,y}\right|^2 = \frac{1}{4\pi^2}\int_{k_y=0}^{2\pi}\int_{k_x=0}^{2\pi}u^{(n)*}_{k_x,k_y}\left(i\frac{d}{dk_x}\right)u^{(n)}_{k_x,k_y}dk_x dk_y = 0$$

$$\begin{aligned}\langle y\rangle_U &= \sum_{x,y} y\left|U^{(n)}_{x,y}\right|^2 = \frac{1}{4\pi^2}\int_{k_y=0}^{2\pi}\int_{k_x=0}^{2\pi} u^{(n)*}_{k_x,k_y}\left(i\frac{d}{dk_y}\right)u^{(n)}_{k_x,k_y}dk_xdk_y \\ &= \left(1-\frac{2}{\pi}\right)n + \frac{1}{8\pi^2}\int_{k_y=0}^{2\pi}\int_{k_x=0}^{2\pi}\frac{\cos^2(k_x)\sin(k_x)\sin(k_y)}{\left(1-\sin^2(k_x)\sin^2(k_y)\right)^{3/2}}\sin\left(2n\arccos\left(\sin(k_x)\sin(k_y)\right)\right)dk_xdk_y\end{aligned}$$

$$\begin{aligned}\langle x^2\rangle_U &= \sum_{x,y} x^2\left|U^{(n)}_{x,y}\right|^2 = \frac{1}{4\pi^2}\int_{k_y=0}^{2\pi}\int_{k_x=0}^{2\pi} u^{(n)*}_{k_x,k_y}\left(i\frac{d}{dk_x}\right)^2 u^{(n)}_{k_x,k_y}dk_xdk_y \\ &= \frac{n^2}{8\pi^2}\int_{k_y=0}^{2\pi}\int_{k_x=0}^{2\pi}\frac{\cos^2(k_x)\sin^2(k_y)\left(1+\sin^2(k_x)\cos(2k_y)\right)}{\left(1-\sin^2(k_x)\sin^2(k_y)\right)^2}dk_xdk_y \\ &+ \frac{n^2}{8\pi^2}\int_{k_y=0}^{2\pi}\int_{k_x=0}^{2\pi}\frac{\cos^4(k_x)\sin^2(k_y)}{\left(1-\sin^2(k_x)\sin^2(k_y)\right)^2}\cos\left(2n\arccos\left(\sin(k_x)\sin(k_y)\right)\right)dk_xdk_y \\ &+ \frac{3n}{8\pi^2}\int_{k_y=0}^{2\pi}\int_{k_x=0}^{2\pi}\frac{\sin(k_x)\sin(k_y)\cos^2(k_x)\cos^2(k_y)}{\left(1-\sin^2(k_x)\sin^2(k_y)\right)^{5/2}}\sin\left(2n\arccos\left(\sin(k_x)\sin(k_y)\right)\right)dk_xdk_y \\ &+ \frac{1}{4\pi^2}\int_{k_y=0}^{2\pi}\int_{k_x=0}^{2\pi}\frac{\sin^2(k_x)\cos^4(k_y)}{\left(1-\sin^2(k_x)\sin^2(k_y)\right)^3}\sin^2\left(n\arccos\left(\sin(k_x)\sin(k_y)\right)\right)dk_xdk_y \\ &- \frac{1}{2\pi^2}\int_{k_y=0}^{2\pi}\int_{k_x=0}^{2\pi}\frac{\sin^2(k_x)\sin^2(k_y)\cos^2(k_x)\cos^2(k_y)}{\left(1-\sin^2(k_x)\sin^2(k_y)\right)^3}\sin^2\left(n\arccos\left(\sin(k_x)\sin(k_y)\right)\right)dk_xdk_y\end{aligned}$$

$$\begin{aligned}\langle y^2\rangle_U &= \sum_{x,y} y^2\left|U^{(n)}_{x,y}\right|^2 = \frac{1}{4\pi^2}\int_{k_y=0}^{2\pi}\int_{k_x=0}^{2\pi} u^{(n)*}_{k_x,k_y}\left(i\frac{d}{dk_y}\right)^2 u^{(n)}_{k_x,k_y}dk_xdk_y \\ &= \frac{n^2}{8\pi^2}\int_{k_y=0}^{2\pi}\int_{k_x=0}^{2\pi}\frac{\sin^2(k_x)\cos^2(k_y)\left(1+\sin^2(k_x)\cos(2k_y)\right)}{\left(1-\sin^2(k_x)\sin^2(k_y)\right)^2}dk_xdk_y \\ &+ \frac{n^2}{8\pi^2}\int_{k_y=0}^{2\pi}\int_{k_x=0}^{2\pi}\frac{\sin^2(k_x)\cos^2(k_x)\cos^2(k_y)}{\left(1-\sin^2(k_x)\sin^2(k_y)\right)^2}\cos\left(2n\arccos\left(\sin(k_x)\sin(k_y)\right)\right)dk_xdk_y \\ &+ \frac{3n}{8\pi^2}\int_{k_y=0}^{2\pi}\int_{k_x=0}^{2\pi}\frac{\cos^4(k_x)\sin(k_x)\sin(k_y)}{\left(1-\sin^2(k_x)\sin^2(k_y)\right)^{5/2}}\sin\left(2n\arccos\left(\sin(k_x)\sin(k_y)\right)\right)dk_xdk_y \\ &- \frac{n}{4\pi^2}\int_{k_y=0}^{2\pi}\int_{k_x=0}^{2\pi}\frac{\cos^2(k_x)\sin(k_x)\sin(k_y)}{\left(1-\sin^2(k_x)\sin^2(k_y)\right)^{3/2}}\sin\left(2n\arccos\left(\sin(k_x)\sin(k_y)\right)\right)dk_xdk_y \\ &+ \frac{3}{4\pi^2}\int_{k_y=0}^{2\pi}\int_{k_x=0}^{2\pi}\frac{\sin^2(k_x)\cos^2(k_x)\cos^2(k_y)}{\left(1-\sin^2(k_x)\sin^2(k_y)\right)^3}\sin^2\left(n\arccos\left(\sin(k_x)\sin(k_y)\right)\right)dk_xdk_y \\ &- \frac{1}{2\pi^2}\int_{k_y=0}^{2\pi}\int_{k_x=0}^{2\pi}\frac{\sin^2(k_x)\cos^2(k_x)\cos^2(k_y)}{\left(1-\sin^2(k_x)\sin^2(k_y)\right)^2}\sin^2\left(n\arccos\left(\sin(k_x)\sin(k_y)\right)\right)dk_xdk_y\end{aligned}$$

In the limit of large n, we have:

$$P_U \to \frac{1}{2} + \frac{1}{8\pi^2}\int_{k_y=0}^{2\pi}\int_{k_x=0}^{2\pi}\frac{\cos^2(k_y)\sin^2(k_x)}{\sin^2\left(\arccos\left(\sin(k_x)\sin(k_y)\right)\right)}dk_xdk_y = 1-\frac{1}{\pi}$$

$$\langle x\rangle_U \to 0$$

$$\langle y \rangle_U \to \left(1 - \frac{2}{\pi}\right) n$$

$$\left\langle x^2 \right\rangle_U \to \frac{n^2}{8\pi^2} \int_{k_y=0}^{2\pi} \int_{k_x=0}^{2\pi} \frac{\cos^2(k_x) \sin^2(k_y) \left(1 + \sin^2(k_x) \cos(2k_y)\right)}{\left(1 - \sin^2(k_x) \sin^2(k_y)\right)^2} dk_x dk_y = \left(1 - \frac{5}{2\pi}\right) n^2$$

$$\left\langle y^2 \right\rangle_U \to \frac{n^2}{8\pi^2} \int_{k_y=0}^{2\pi} \int_{k_x=0}^{2\pi} \frac{\sin^2(k_x) \cos^2(k_y) \left(1 + \sin^2(k_x) \cos(2k_y)\right)}{\left(1 - \sin^2(k_x) \sin^2(k_y)\right)^2} dk_x dk_y = \left(1 - \frac{13}{6\pi}\right) n^2$$

For the first few steps, we have:

$$u^{(0)}_{k_x,k_y} = 1 \to U^{(0)}_{x,y} = \delta(x)\,\delta(y)$$

$$u^{(1)}_{k_x,k_y} = ie^{-ik_y} \sin(k_x) \to U^{(1)}_{x,y} = \begin{cases} 0.5\,(x=-1, y=1) \\ -0.5\,(x=1, y=1) \\ 0\,(Otherwise) \end{cases}$$

$$u^{(2)}_{k_x,k_y} = -e^{-ik_y} \left(\cos(k_y) + i\cos(2k_x)\sin(k_y)\right) \to U^{(2)}_{x,y} = \begin{cases} -0.25\,(x=-2, y=0) \\ -0.5\,(x=0, y=0) \\ -0.25\,(x=2, y=0) \\ 0.25\,(x=-2, y=2) \\ -0.5\,(x=0, y=2) \\ 0.25\,(x=2, y=2) \\ 0\,(Otherwise) \end{cases}$$

$$u^{(3)}_{k_x,k_y} = ie^{-ik_y} \sin(k_x) \left(\cos(2k_x)\cos(2k_y) - 2\cos^2(k_x) + i\sin(2k_y)\right) \to U^{(3)}_{x,y} = \begin{cases} 0.125\,(x=-3, y=-1) \\ 0.125\,(x=-1, y=-1) \\ -0.125\,(x=1, y=-1) \\ -0.125\,(x=3, y=-1) \\ -0.25\,(x=-3, y=1) \\ -0.25\,(x=-1, y=1) \\ 0.25\,(x=1, y=1) \\ 0.25\,(i=3, y=1) \\ 0.125\,(x=-3, y=3) \\ -0.375\,(x=-1, y=3) \\ 0.375\,(x=1, y=3) \\ -0.125\,(x=3, y=3) \\ 0\,(Otherwise) \end{cases}$$

These are consistent with what we expect from recursive analysis of the evolution.

B. Time-independent phase modulation:

Uniform modulation

For the case of time-independent linear phase modulation, $\phi_{n,y} = y\phi$, we have:

$$\begin{bmatrix} s^{(n+1)}_{k_x,k_y} \\ p^{(n+1)}_{k_x,k_y} \end{bmatrix} = \begin{bmatrix} ie^{-ik_x}\sin(k_y) & e^{ik_x}\cos(k_y) \\ -e^{-ik_x}\cos(k_y) & -ie^{ik_x}\sin(k_y) \end{bmatrix} \begin{bmatrix} s^{(n)}_{k_x,k_y+\phi} \\ p^{(n)}_{k_x,k_y-\phi} \end{bmatrix}$$

For rational values of $\phi/2\pi = p/q$, we can consider s_{k_x,k_y}, $s_{k_x,k_y+\phi}$, $s_{k_x,k_y+2\phi}$, ..., $s_{k_x,k_y+(q-1)\phi}$ as well as p_{k_x,k_y}, $p_{k_x,k_y+\phi}$, $p_{k_x,k_y+2\phi}$, ..., $p_{k_x,k_y+(q-1)\phi}$ together as a vector. Then we can obtain the evolution equation for this vector. Note that this approach does not work for irrational values of $\phi/2\pi$. By representing this vector as

$$\psi^{(n)} = \begin{bmatrix} s^{(n)}_{k_x,k_y} & s^{(n)}_{k_x,k_y+\phi} & \cdots & s^{(n)}_{k_x,k_y+(q-1)\phi} & p^{(n)}_{k_x,k_y} & p^{(n)}_{k_x,k_y+\phi} & \cdots & p^{(n)}_{k_x,k_y+(q-1)\phi} \end{bmatrix}^T,$$

we can write the evolution equation as:

$$\psi^{(n+1)} = M(k_x,k_y)\,\psi^{(n)}$$

In this equation, M is the evolution matrix and its size linearly increases with increasing q.
For a general propagation matrix, the eigen-energies can be calculated from the following characteristic equation:

$$\left|M - e^{iE}I\right| = 0$$

For instance, the evolution matrix for the case of $\phi = \pi$ is given by:

$$M = \begin{bmatrix} 0 & ie^{-ik_x}\sin(k_y) & 0 & e^{ik_x}\cos(k_y) \\ ie^{-ik_x}\sin(k_y+\pi) & 0 & e^{ik_x}\cos(k_y+\pi) & 0 \\ 0 & -e^{-ik_x}\cos(k_y) & 0 & -ie^{ik_x}\sin(k_y) \\ -e^{-ik_x}\cos(k_y+\pi) & 0 & -ie^{ik_x}\sin(k_y+\pi) & 0 \end{bmatrix}$$

In this case, the eigen-energies are given by:

$$E(k_x,k_y) = \pm\arccos\left(\pm\sqrt{1-\sin^2(k_x)\sin^2(k_y)}\right)$$

Similar expressions can be obtained for other phase modulations. The obtained band diagrams for different values of ϕ are shown in Fig. S2.

Considering the evolution of the quantum walk under the effect of time-independent gauge fields, Fig. S3 summarizes the numerical results for the variation of the quadratic means with the time step for different values of ϕ. The obtained results show that the applied gauge fields cause the quadratic means of x and y to decrease relative to the zero phase modulation case. These numerical results are obtained using the quantum walk distributions determined according to the pulses detected in the down channel. However, the quadratic means are normalized relative to the total power in the up and down channels in Figs. S3a and S3b. The corresponding quadratic means normalized to the total power in the down channel are shown in Figs. S3c and S3d. Moreover, these quadratic means are also plotted for just the first 10 steps in Figs. S3e and S3f.

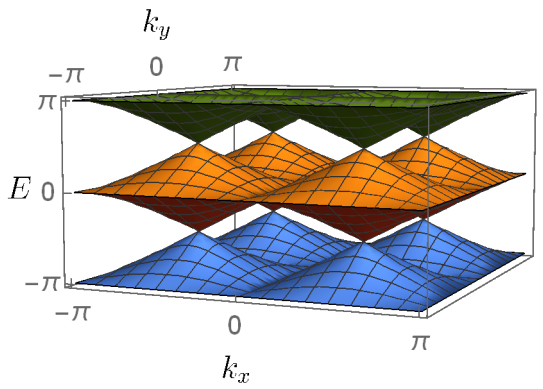

(a)

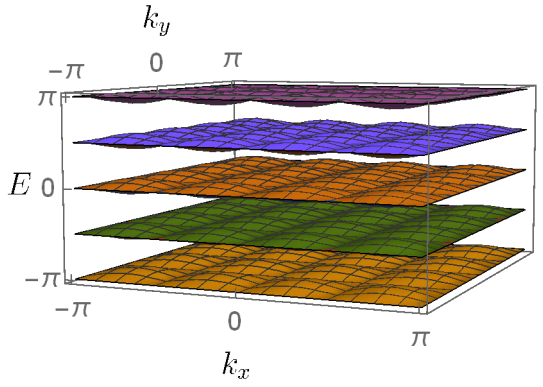

(b)

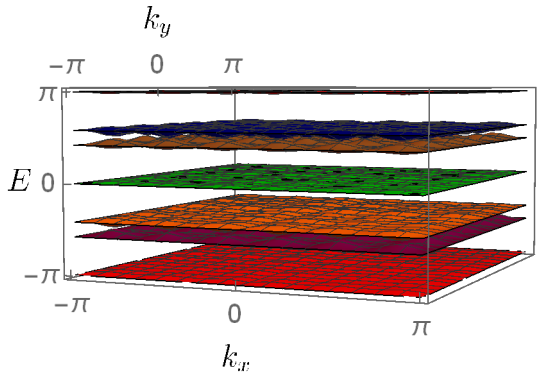

(c)

Figure S2. The energy band diagrams for the time-independent phase modulation with (a) $\phi = \pi$, (b) $\phi = \pi/2$, and (c) $\phi = \pi/3$.

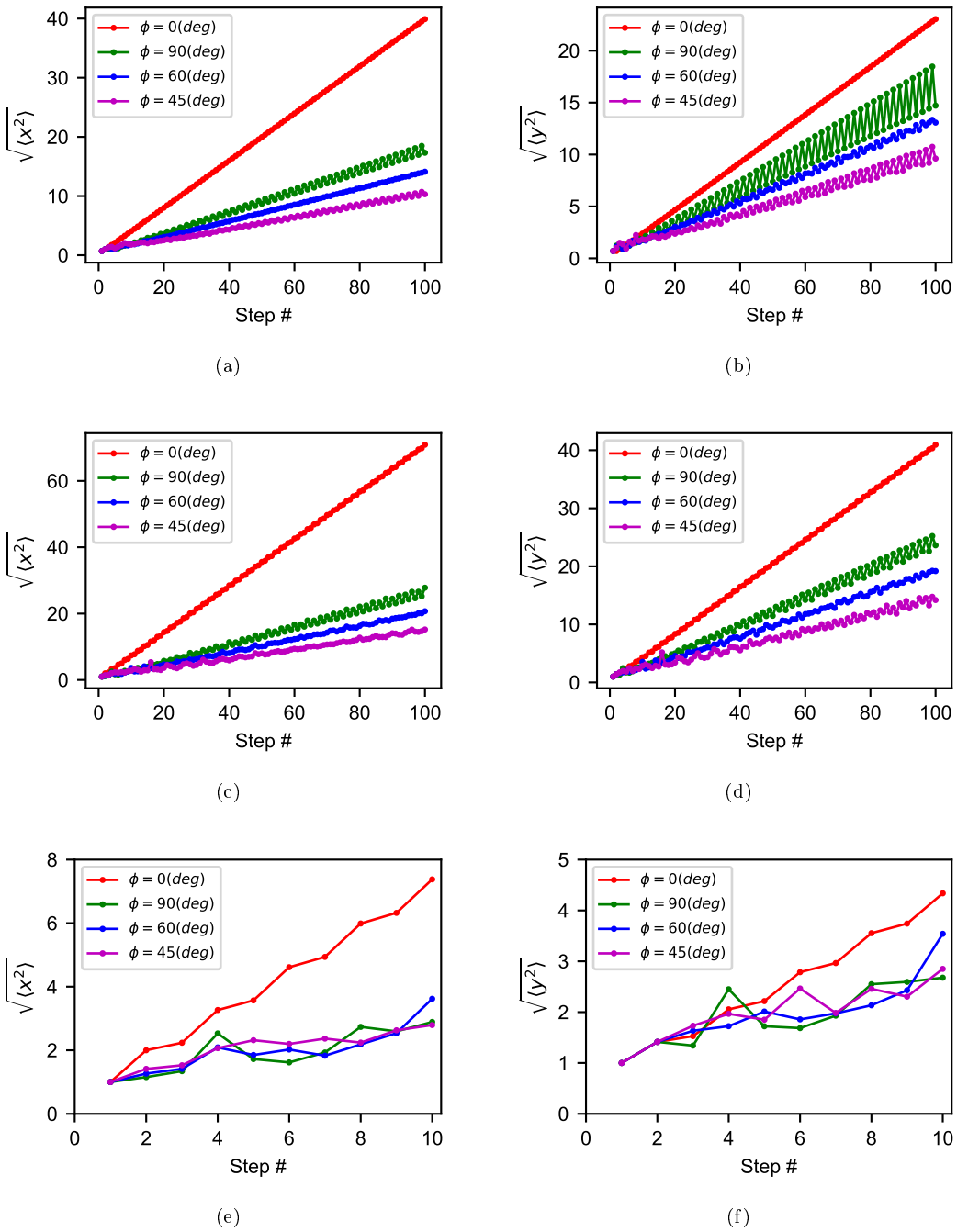

Figure S3. (a) The quadratic mean of x and (b) y as a function of the time step for different values of phase modulations. These quadratic means are normalized relative to the total power in the up and down channels. (c) The quadratic mean of x and (d) y as a function of the time step for different values of phase modulations. These quadratic means are normalized relative to the total power in the down channel. (e) The quadratic mean of x and (f) y for different values of phase modulations for the first 10 time steps.

Non-uniform modulation

We next consider the case in which the phase modulation pattern changes across a boundary. This type of phase modulation can lead to the emergence of the edge states right along the boundary. We have assumed $y = 0$ as the boundary separating two time-independent linear phase modulations in $y > 0$ and $y < 0$. Since we do not have

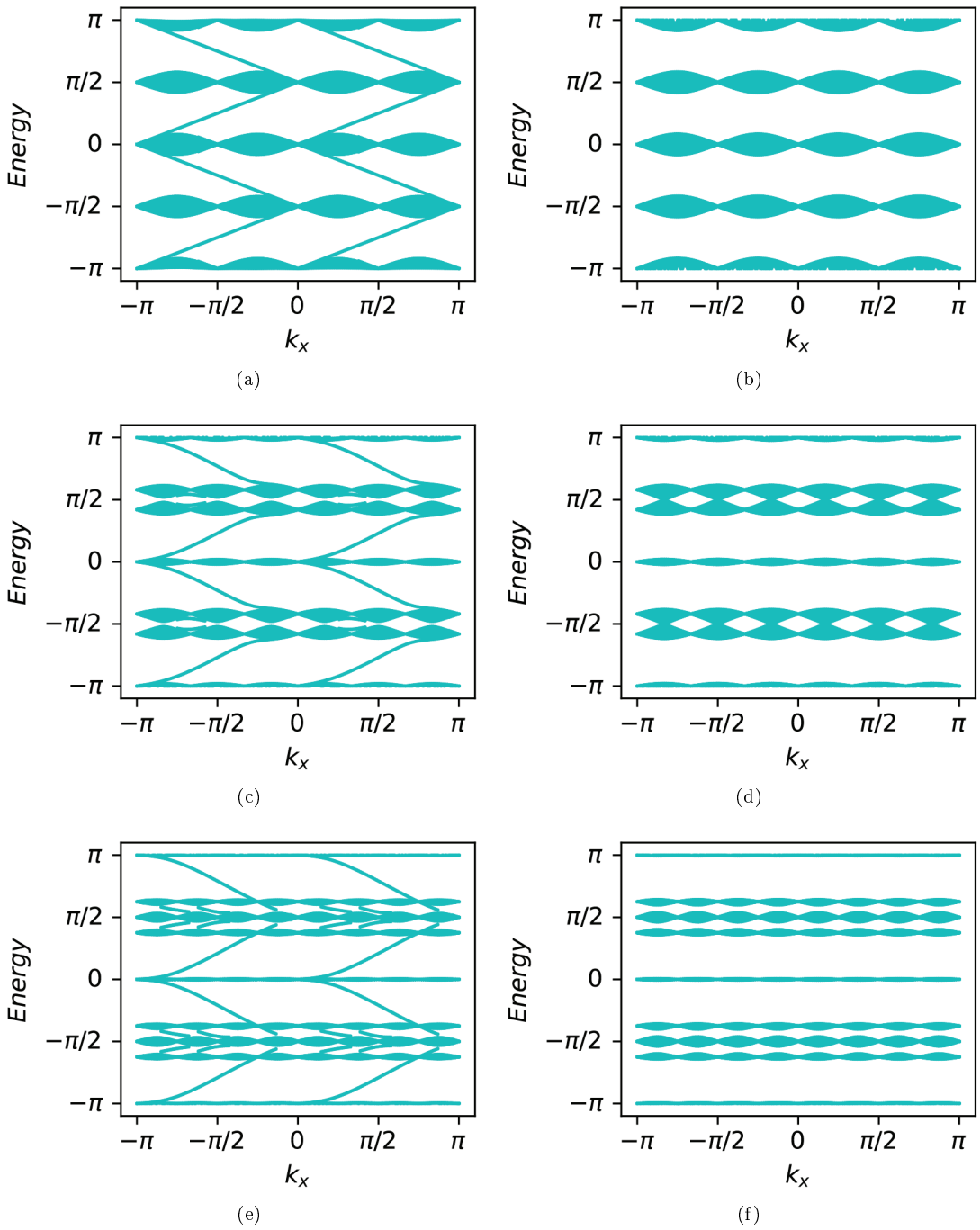

Figure S4. The left panel shows the energy band diagrams for the time-independent non-uniform phase modulations of (a) $\phi_T = -\phi_B = \pi/2$, (c) $\phi_T = -\phi_B = \pi/3$, and (e) $\phi_T = -\phi_B = \pi/4$. The right panel shows the corresponding band diagrams for the uniform phase modulations of (b) $\phi_T = \phi_B = \pi/2$, (d) $\phi_T = \phi_B = \pi/3$, and (f) $\phi_T = \phi_B = \pi/4$.

translational symmetry in the y direction anymore, we cannot define k_y for this configuration. However, we can still obtain the allowed eigen-energies for different k_x values. In order to obtain these eigen-energies, we should obtain the propagation matrix in the real space under the appropriate boundary conditions. Depending on the phase modulations at the top (ϕ_T) and the bottom (ϕ_B), we obtain different band diagrams. Numerical results show that if one of ϕ_T and ϕ_B be zero then there exists no edge state. Moreover, the edge states exist only if $0 < \phi_T < \pi \,\&\, -\pi < \phi_B < 0$ or $0 < \phi_B < \pi \,\&\, -\pi < \phi_T < 0$.

We have plotted the energy band diagrams as functions of k_x momentum for different ϕ_T and ϕ_B in Fig. S4. In

this figure, we have considered different cases of $\phi_T = -\phi_B$ as non-uniform configurations with a boundary separating two different linear phase modulations. Note that swapping the values of ϕ_T with ϕ_B will modify the band diagram by replacing the edge states with the ones that propagate in the reverse direction. We have also shown the band diagrams corresponding to uniform modulations with $\phi_B = \phi_T$ for comparison.

Robustness of the edge modes against sharp bends

In order to analyze the robustness of the edge modes against sharp bends, we have studied the propagation of the quantum walk in the synthetic space composed of two domains with opposite gauge fields separated by a nonplanar interface. Similar to the case considered in Fig. 4 in the manuscript, a phase pattern of $\pi y/2$ is applied to the region on top of the boundary and a phase pattern of $-\pi y/2$ is applied to the region below the boundary. However, the boundary, as shown by the dashed lines in Fig. S5, is deformed by a bump relative to the planar boundary considered in the manuscript. The coordinates of the bump are assumed as $(-1, 0)$, $(-1, 4)$, $(-5, 4)$, and $(-5, 0)$ in this analysis. Starting with a unity pulse at the origin in the up channel, we have studied the propagation of the quantum walk and have plotted its distribution in the down channel at different time steps in Fig. S5. In spite of the presence of the bump, as this figure shows, the quantum walk distribution remains confined to the boundary and moves along it in both forward and backward directions. Moreover, the speed of the movement along the boundary is 0.5 irrespective of the shape of the boundary, which is equal to what we expect from the group velocity of the topological edge modes based on the dispersion diagram. These results confirm the robustness of the edge modes against sharp bends.

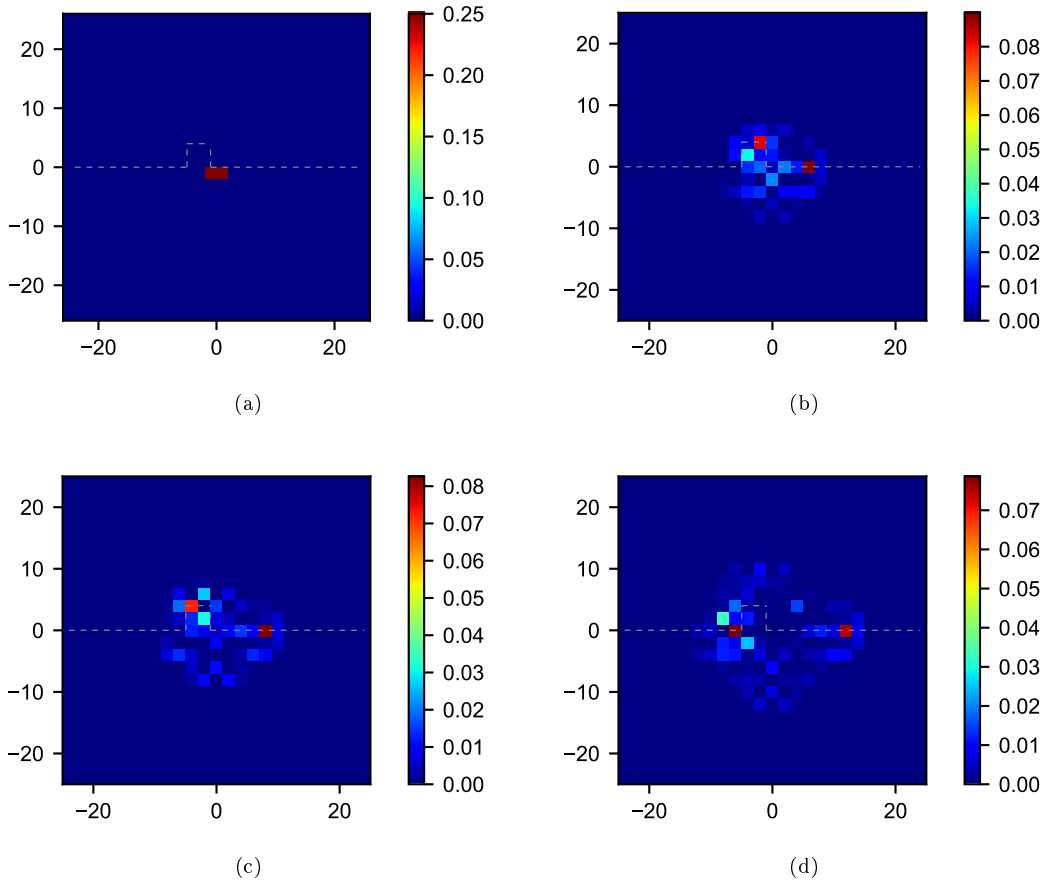

Figure S5. The quantum walk distribution in the down channel after (a) 1, (b) 12, (c) 16, and (d) 24 time steps. These distributions clearly show how the quantum walk moves along the boundary and remains confined to it in spite of its nonplanar shape.